Title

Proteomic Analysis of the Human Tankyrase Protein Interaction Network Reveals Its Role in Pexophagy

Journal

Cell Reports, 20(3)

ISSN

2639-1856

Authors

Li, Xu
Han, Han
Zhou, Mao-Tian
et al.

Publication Date

2017-07-01

DOI

10.1016/j.celrep.2017.06.077

Cell Reports

Resource

Proteomic Analysis of the Human Tankyrase Protein Interaction Network Reveals Its Role in Pexophagy

Graphical Abstract

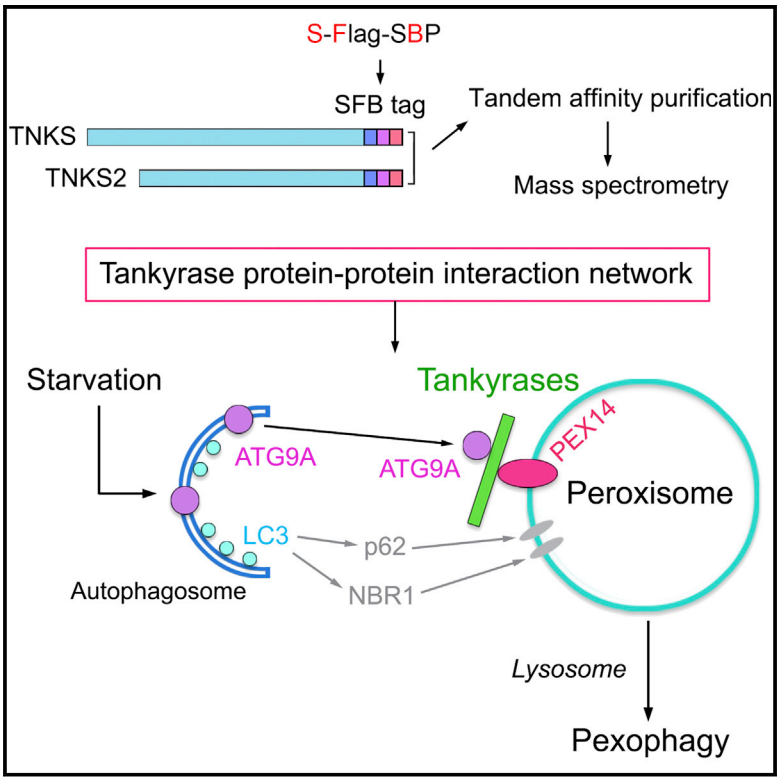

Authors

Xu Li, Han Han, Mao-Tian Zhou, ..., Nan Li, Junjie Chen, Wenqi Wang

Correspondence

jchen8@mdanderson.org (J.C.), wenqiw6@uci.edu (W.W.)

In Brief

Li at al. establish a protein-protein interaction network for human TNKS and TNKS2, two poly(ADP-ribose) polymerase family proteins. They examine and validate the peroxisomal localization of these tankyrases and link them to peroxisome homeostasis.

Highlights

- Proteomic analysis defines the human TNKS and TNKS2 protein-protein interaction network
- TNKS and TNKS2 localize to peroxisomes
- TNKS and TNKS2 associate with PEX14 and ATG9A and promote pexophagy

Accession Numbers

PXD004647

Li et al., 2017, Cell Reports *20*, 737–749
July 18, 2017
http://dx.doi.org/10.1016/j.celrep.2017.06.077

CellPress

Cell Reports
Resource

Proteomic Analysis of the Human Tankyrase Protein Interaction Network Reveals Its Role in Pexophagy

Xu Li,[1,3] Han Han,[2,3] Mao-Tian Zhou,[1,3] Bing Yang,[2] Albert Paul Ta,[2] Nan Li,[1] Junjie Chen,[1,*] and Wenqi Wang[2,4,*]
[1]Department of Experimental Radiation Oncology, The University of Texas MD Anderson Cancer Center, Houston, TX 77030, USA
[2]Department of Developmental and Cell Biology, University of California, Irvine, Irvine, CA 92697, USA
[3]These authors contributed equally
[4]Lead Contact
*Correspondence: jchen8@mdanderson.org (J.C.), wenqiw6@uci.edu (W.W.)
http://dx.doi.org/10.1016/j.celrep.2017.06.077

SUMMARY

Tankyrase 1 (TNKS) and tankyrase 2 (TNKS2) belong to the poly(ADP-ribose) polymerase family of proteins, which use nicotinamide adenine dinucleotide to modify substrate proteins with ADP-ribose modifications. Emerging evidence has revealed the pathological relevance of TNKS and TNKS2, and identified these two enzymes as potential drug targets. However, the cellular functions and regulatory mechanisms of TNKS/2 are still largely unknown. Through a proteomic analysis, we defined the protein-protein interaction network for human TNKS/2 and revealed more than 100 high-confidence interacting proteins with numerous biological functions in this network. Finally, through functional validation, we uncovered a role for TNKS/2 in peroxisome homeostasis and determined that this function is independent of TNKS enzyme activities. Our proteomic study of the TNKS/2 protein interaction network provides a rich resource for further exploration of tankyrase functions in numerous cellular processes.

INTRODUCTION

The poly(ADP-ribose) polymerase (PARP) protein superfamily is a group of enzymes that use nicotinamide adenine dinucleotide (NAD^+) as a substrate to modify target proteins by adding ADP-ribose modifications (Berger et al., 2004; Bürkle, 2005; Riffell et al., 2012). This post-translational modification, called PARylation, plays crucial roles in various cellular functions, including DNA damage repair (Malanga and Althaus, 2005), apoptosis (Koh et al., 2005), stress response (Leung et al., 2011), cell division (Chang et al., 2004), transcription (Kraus and Lis, 2003), and chromatin remodeling (Schreiber et al., 2006). The 17 identified members of the PARP family, which have structurally similar PARP catalytic domains (Amé et al., 2004; Hottiger et al., 2010; Rouleau et al., 2010; Vyas et al., 2013), have diverse cellular localizations and functions. Among them, PARP1 and PARP2 have been the main foci of research because pharmacologically targeting their enzyme activities interferes with DNA damage repair (Durkacz et al., 1980, 1981b) and sensitizes cells to the effects of DNA-damaging agents (Durkacz et al., 1981a). Recent studies have also highlighted the potential of two additional druggable PARP family members, tankyrase 1 (TNKS) and tankyrase 2 (TNKS2), as therapeutic targets (Lehtiö et al., 2013; Riffell et al., 2012).

Mice with knockout of either TNKS or TNKS2 are viable and display only a mild phenotype, but loss of both tankyrases leads to embryonic lethality (Chiang et al., 2008), suggesting that TNKS and TNKS2 are functionally redundant. Indeed, TNKS and TNKS2 share high sequence identity. TNKS contains four distinct domains: an *N*-terminal homopolymeric region with His, Pro, and Ser residues (His-Pro-Ser domain); an ankyrin domain containing 5 ankyrin repeat clusters (ARCs) for 24 ankyrin repeats; a sterile alpha module (SAM) domain; and a C-terminal PARP catalytic domain (Lehtiö et al., 2013). TNKS2 lacks the N-terminal His-Pro-Ser domain but has an extra seven-residue insertion between the ARCs and the SAM domain (Lehtiö et al., 2013). In addition, TNKS and TNKS2 can associate with each other through their SAM domains, facilitating their PARP activities and cellular functions (Lehtiö et al., 2013; Mariotti et al., 2016).

The association between TNKS/2 and their substrates is mediated by their ankyrin domains and a short consensus amino acid sequence, RxxPxG, in the substrates (Guettler et al., 2011; Morrone et al., 2012). The relatively long ankyrin domains of TNKS/2 can serve as docking sites for the substrates, giving TNKS/2 a large capacity to bind a variety of substrates (Lehtiö et al., 2013). Moreover, a database search revealed that hundreds of human proteins contain the RxxPxG motif or its degenerated form; these proteins could be substrates for TNKS/2 (Guettler et al., 2011).

The TNKS-mediated PARylation of substrates leads to two possible outcomes: a change in their localization or proteasome-dependent degradation. The E3 ligase RNF146 recognizes the PARylation of TNKS substrates and is responsible for their subsequent ubiquitination and degradation (Zhang et al., 2011). Functionally, TNKS and TNKS2 control various cellular events through their corresponding substrates. For example, TNKS and TNKS2 regulate telomere homeostasis by binding to and degrading the telomere protein TRF1 (Smith et al., 1998). TNKS and TNKS2 also activate Wnt signaling by degrading the β-catenin destruction complex components AXIN1 and AXIN2 (Huang et al., 2009). Moreover, TNKS and TNKS2 associate with and PARylate the NUMA protein at spindle poles to regulate mitotic checkpoint (Chang et al., 2005), positively regulate the AKT pathway by degrading the tumor suppressor PTEN (Li et al., 2015), and are involved in the heritable disease cherubism

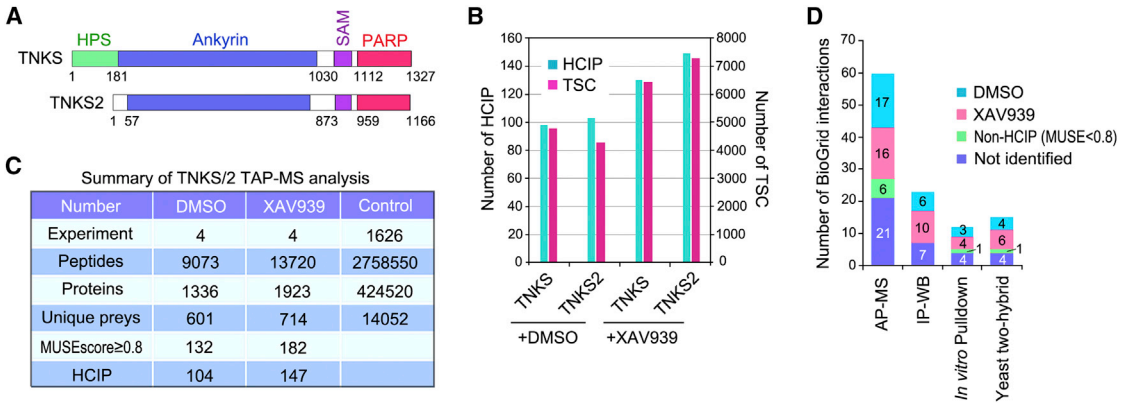

C

Summary of TNKS/2 TAP-MS analysis

Number	DMSO	XAV939	Control
Experiment	4	4	1626
Peptides	9073	13720	2758550
Proteins	1336	1923	424520
Unique preys	601	714	14052
MUSEscore≥0.8	132	182	
HCIP	104	147	

Figure 1. Proteomic Analysis of the TNKS/2 Protein Interaction Network

(A) Schematic illustration of human TNKS and TNKS2 protein domains.

(B) The total spectral counts (TSCs) and corresponding numbers of HCIPs for TNKS and TNKS2 under the indicated treatments.

(C) Total numbers of peptides and proteins identified in the MS analysis. A MUSE score $\geq$0.8 was used as the cutoff to identify HCIPs.

(D) Comparison of the numbers of TNKS/2-interacting proteins identified using AP-MS, immunoprecipitation-western blotting (IP-WB), in vitro pulldown assay, and yeast two-hybrid in the BioGrid database with the interacting proteins found in our dataset.

See also Figure S1 and Tables S1, S2, S3, and S4.

by regulating the protein stability of 3BP2 (Levaot et al., 2011). Recently, we and others demonstrated that TNKS and TNKS2 play a positive role in the regulation of YAP, a key downstream effector in the Hippo pathway, by degrading the angiomotin (AMOT) family of proteins (Troilo et al., 2016; Wang et al., 2015, 2016). Because some of the substrates that are PARylated and degraded by TNKS/2 are tumor suppressors—for example, AXIN1/2, PTEN, and AMOTs—TNKS/2 could be attractive targets for cancer therapy. Indeed, researchers have developed TNKS/2 inhibitors and demonstrated them to be effective anticancer agents (Lehtiö et al., 2013; Riffell et al., 2012), indicating that TNKS/2 inhibition has great translational potential.

Previous studies have not only highlighted the important roles of TNKS/2 in maintaining tissue homeostasis and their potential usefulness in cancer therapy, but also fueled a great interest in identifying additional TNKS/2 binding partners. To further elucidate the biological functions and therapeutic potential of TNKS/2, we conducted a proteomic analysis of TNKS/2-associated protein complexes in both normal and inactive conditions. By using the Minkowski distance-based unified scoring environment (MUSE) algorithm (Li et al., 2016), we identified 104 and 147 high-confidence interacting proteins (HCIPs) under normal and TNKS/2-inactive conditions, respectively. Through in-depth functional validation, we demonstrated the association of peroxisome protein 14 (PEX14) and TNKS/2, and further characterized the role of TNKS/2 in pexophagy. Our proteomic study not only elucidated the TNKS/2 protein-protein interaction network, but also revealed a number of previously uncharacterized binding partners and potential substrates for TNKS/2.

RESULTS

Proteomic Analysis of the Protein-Protein Interaction Network for TNKS/2

To achieve a comprehensive understanding of the TNKS/2 protein interaction network, we established HEK293T cells stably expressing human TNKS or TNKS2 (Figure 1A) fused with SFB triple tags (S tag-FLAG tag-streptavidin-binding peptide [SBP] tag) through viral infection and puromycin selection (Figures S1A and S1B). After validation by western blotting and immunofluorescent staining, we subjected these TNKS-293T and TNKS2-293T cells to tandem affinity purification (TAP) (Figure S1A). To determine whether TNKS/2 enzyme activities are required for protein complex formation, we pretreated the cells with the TNKS/2 inhibitor XAV939 for 48 hr. XAV939 has been shown to dramatically suppress TNKS/2 activities (Wang et al., 2015). Cells pretreated with DMSO were used as controls (Figure S1A). We identified the associated proteins in the isolated complexes using mass spectrometry (MS) and matched them with proteins in the human International Protein Index database. A complete list of the peptides and proteins identified is provided in Table S1.

To refine the TNKS/2 proteomic data, we used the MUSE algorithm, which has been described previously (Li et al., 2016), to assign quality scores to the identified protein-protein interactions. To filter out nonspecific interacting proteins, we applied a control group of 1,626 unrelated TAP-MS experiments that were performed under identical experimental conditions (1,606 experiments using overexpressed TAP-tagged protein baits and 20 experiments using empty vector baits) to the MUSE algorithm. We assigned a MUSE score to each identified interaction and considered any interaction with a MUSE score of least 0.8 and raw spectra counts greater than 1 to be an HCIP (Figure S1A). Through these analyses, we identified 104 HCIPs among the 601 unique preys of TNKS/2 proteins in the DMSO-treated control group and 147 HCIPs among the 714 identified unique preys in the XAV939-treated group (Figures 1B and 1C; Tables S2, S3, and S4). In addition, a subset of the above-mentioned 1,626 controls, which contains 338 TAP-MS experiments whose raw data are available in the PRIDE database, were used as our secondary control set for the MUSE analysis, where 91% of identified HCIPs were confirmed (Tables S3 and

S4). This evaluation suggests that our current data analysis is highly reproducible by using a publicly available control set. To estimate the frequently observed non-specific binding proteins in our HCIPs, we compared our HCIP dataset with the Contaminant Repository for Affinity Purification (CRAPome), a well-designed repository of ''frequent flyers'' for affinity purification (Mellacheruvu et al., 2013). Only 5.6% of our identified HCIPs overlapped with the preys frequently shown in the CRAPome database (i.e., >20% frequency). 92.8% of HCIPs were enriched at least 5-fold, whereas 87.3% of HCIPs were enriched at least 20-fold in comparison with their respective abundances in the CRAPome database (Table S4). Again, these results highlight the quality of our TNKS HCIP dataset.

Overview of the TNKS Protein Interaction Network

To determine the reproducibility of our TAP data, we performed biological replication for all of the experiments. The overall HCIP reproducibility rate was close to 90%, and this rate increased when the cutoff number of identified peptides increased, suggesting that our proteomic data were highly reproducible. TNKS and TNKS2 had more than 85% overlap in their HCIPs (Figure S1C), indicating that their binding proteins are quite similar, so we combined them for further bioinformatic analysis. Intriguingly, although treatment with XAV939 inhibited the enzyme activity of TNKS/2, the identified HCIPs in the XAV939-treated group substantially overlapped with the ones identified in the DMSO-treated control group (Figure S1C; Table S5), suggesting that TNKS/2 enzyme activities have only a mild effect on the formation of the TNKS/2 protein interaction complex under these experimental conditions.

We next compared our HCIP lists with data available in the literature. Of 60 protein interactions identified using high-throughput affinity purification (AP)-MS experiments with TNKS/2 and reported in BioGrid, 17 were identified as HCIPs in the DMSO-treated control group and 16 in the XAV939-treated group (Figure 1D). Of 23 interactions identified using immunoprecipitation-western blotting (IP-WB), 6 were identified as HCIPs in the DMSO-treated control group and 10 were identified as HCIPs in the XAV939-treated group (Figure 1D). Of 12 interactions reported in BioGrid and identified in in vitro pulldown experiments with TNKS/2, 3 were identified as HCIPs in the DMSO-treated control group and 4 were identified in the XAV939-treated group (Figure 1D). Finally, for yeast two-hybrid data in BioGrid, we identified 4 out of 15 reported interactions with TNKS/2 in the DMSO group and 6 out of 15 in the XAV939 group (Figure 1D). Several of the interactions reported in BioGrid were also identified in our dataset but did not pass the stringent filtering criteria we used with the MUSE algorithm (six interactions in AP-MS, one interaction in in vitro pulldown, and one interaction in yeast two-hybrid data). Moreover, we identified additional high-confidence interactions with TNKS/2 that were not reported in BioGrid (Figure 1D), further extending our knowledge of the TNKS/2 protein interactome. Taken together, these results suggest that our TNKS/2 proteomic dataset not only reproduced previous findings, but also provided an additional collection of candidate HCIPs for further validation.

To provide a comprehensive overview of the cellular functions that TNKS/2 may be involved in, we performed Gene Ontology (GO) analysis of the TNKS/2 HCIPs. This analysis indicated that the identified HCIPs have different subcellular localizations (Figure S1D) and are involved in multiple cellular functions (Figure S1E). We also conducted a signaling pathway annotation for TNKS/2 HCIPs. Besides the reported pathways (i.e., telomere regulation, Wnt-β catenin pathway, and Hippo pathway), several other key signaling pathways were also highly enriched (i.e., hypoxia signaling, Rho GTPase signaling, and autophagy), suggesting that TNKS and TNKS2 have more extensive cellular functions than previously reported (Figure S1F; Table S6).

We also organized the TNKS/2 protein interaction network globally and functionally, focusing on clustering the HCIPs based on their subcellular localizations or biological functions (Figure 2). TNKS/2 HCIPs were enriched in several organelles, such as the mitochondria, Golgi apparatus, endoplasmic reticulum, peroxisomes, endosomes, plasma membrane, centrosomes, and cytoskeleton (actin and tubulin) (Figure 2). Moreover, GO analysis specifically pointed to two protein families that may be associated with TNKS/2: the STRIPAK protein phosphatase complex and an E3 ligase group that includes RNF146, which degrades TNKS substrates (Figure 2). Taken together, these data suggested that TNKS and TNKS2 localize on several cellular compartments and may participate in biological processes related to these organelles.

To validate the TNKS/2 protein interaction network, we performed reciprocal TAP-MS with 10 selected HCIPs (SSSCA1, BCR, GSK3β, STRN, STRN3, PDCD10, CTNNBPL2, FAM40A, PEX5, and PEX14). Among these, we reciprocally identified TNKS/2 in SSSCA1, BCR, STRN3, and PEX14 TAP-MS experiments (Figure 3A), which were also identified previously (Guettler et al., 2011). As shown in Figures 3B and 3C, SSSCA1 associates with both TNKS and TNKS2. We also validated the interaction between BCR and TNKS (Figure 3D). The TNKS/2 TAP-MS experiments identified many subunits of the STRIPAK protein phosphatase complex (Figure 2); however, a strong interaction was detected only between STRN3 and TNKS (Figure 3E), suggesting that STRN3 is the major TNKS binding partner in this stable complex. In addition, both TNKS and TNKS2 are associated with STRN3 (Figure 3F). These data were consistent with the results of the reciprocal TAP-MS, in which STRN3, but not STRN, PDCD10, CTNNBPL2, or FAM40A in the STRIPAK complex, reciprocally identified TNKS/2.

Even though GSK3β-reciprocal TAP-MS did not identify TNKS/2, we detected interactions between GSK3β and TNKS/2 by co-transfection followed by IP-WB experiments (Figure 3G). GSK3β can phosphorylate TNKS/2 during mitosis, but the function of this phosphorylation is not clear (Yeh et al., 2006). This may explain why we did not identify TNKS/2 in the GSK3β-reciprocal TAP-MS experiment, because most kinase-substrate interactions are transient and weak. To determine the role of GSK3β in TNKS/2 regulation, we treated cells with the GSK3β inhibitor LiCl and found that LiCl-mediated inhibition of GSK3β decreased TNKS protein levels (Figure 3H). Intriguingly, LiCl treatment decreased both TNKS and TNKS2 protein levels when TNKS/2 enzyme activities were inhibited by XAV939, but had only a mild effect on expression level of the TNKS/2 substrate AMOT (Figure 3I). These data suggested

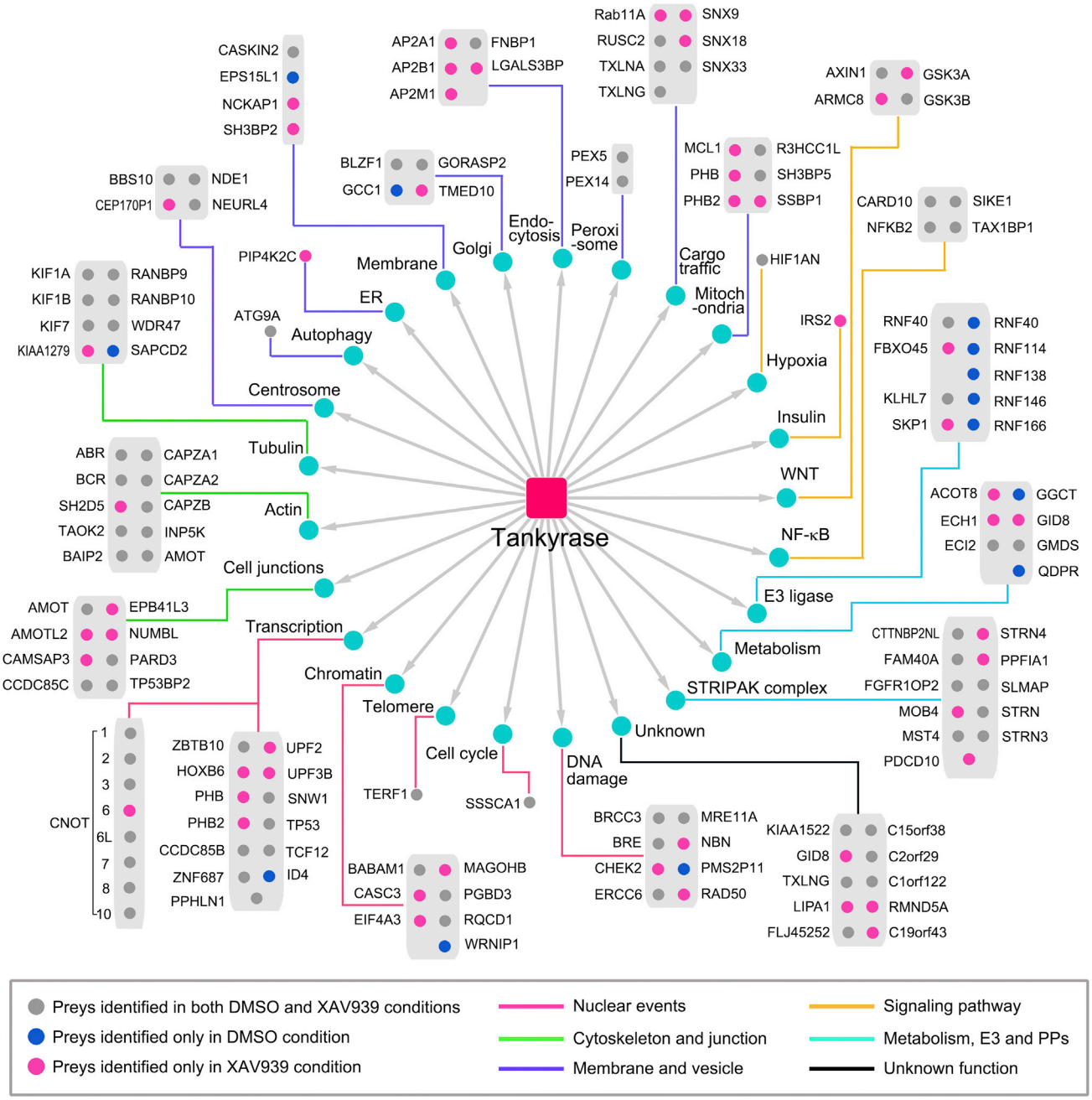

Figure 2. Integrated Interaction Map of the Human TNKS/2 Family

TNKS/2 HCIPs were grouped based on their cellular functions and localizations as indicated by GO analysis and a literature search. The different dot colors indicate the dependencies of the HCIPs on XAV939-based treatment. ER, endoplasmic reticulum. See also Tables S4, S5, and S6.

that GSK3β might stabilize TNKS/2. The functional relevance of these findings deserves further investigation.

TNKS and TNKS2 Interact with the Peroxisome Protein PEX14

In our proteomic analysis, we identified two peroxisome proteins, PEX5 and PEX14, as TNKS/2-associated proteins (Figure 2). PEX5 and PEX14 form a heterodimer that facilitates cytosolic cargo docking and transport into the peroxisome lumen (Brocard et al., 1997; Smith and Aitchison, 2013). Consistent with the results of our reciprocal TAP-MS validation of the TNKS protein interaction network, we found that TNKS specifically interacted with PEX14, but not PEX5 (Figure 3J). Moreover, PEX14 interacted with both TNKS and TNKS2 (Figure 3K). TNKS enzyme activity was not required for its association with PEX14, because the TNKS PAR-inactive mutant TNKS-PD still bound to

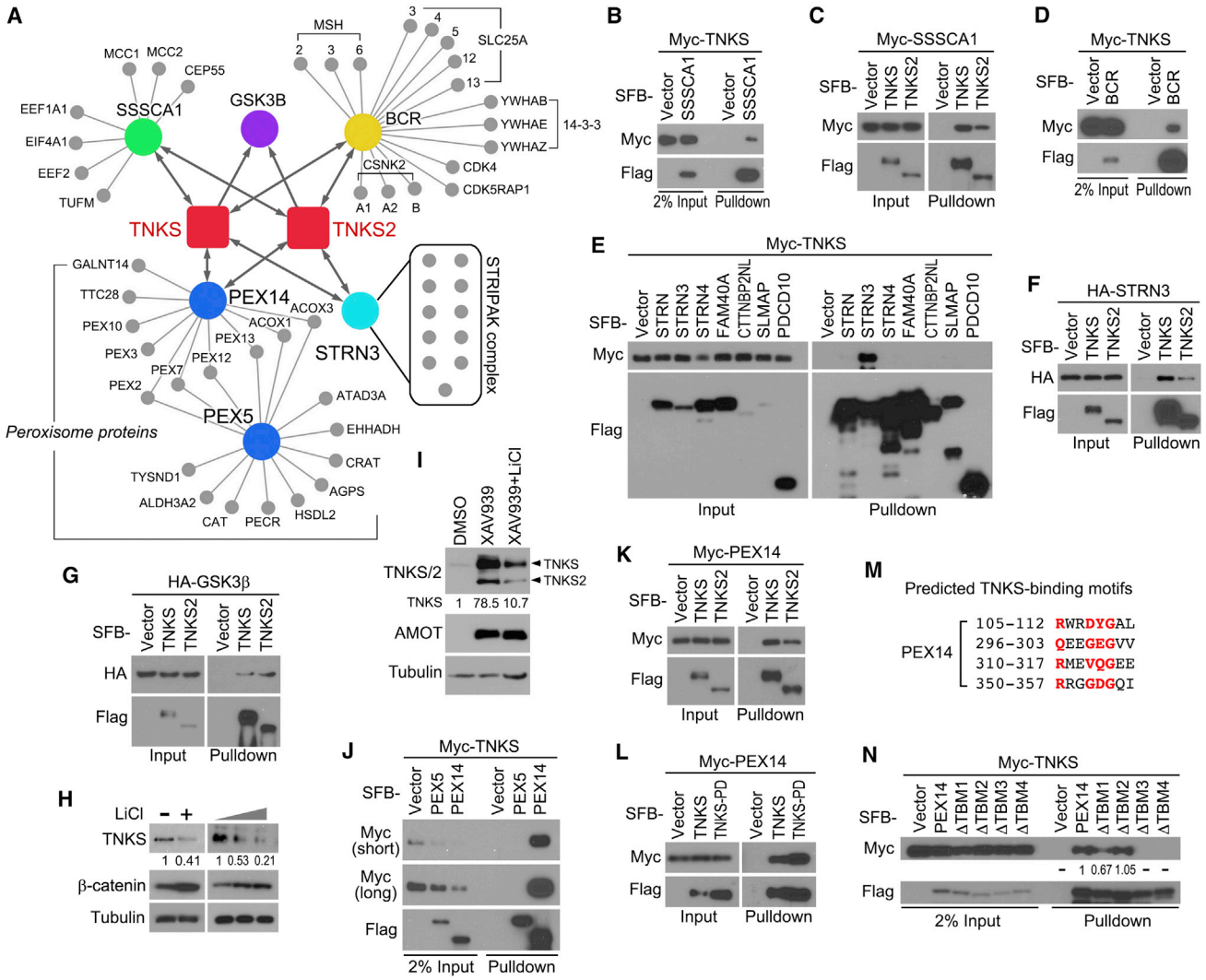

Figure 3. Validation of TNKS/2 Proteomics

(A) A summary map of cytoscape-generated merged interaction network for TNKS/2 and selected reciprocal HCIPs.

(B) SSSCA1 interacts with TNKS. A pulldown assay was performed with S protein beads (SFB-tagged proteins were used as the baits), and the indicated proteins were detected by WB.

(C) Association between TNKS/2 and SSSCA1. A pulldown assay was performed with S protein beads (SFB-tagged proteins were used as the baits), and the indicated proteins were detected by WB.

(D) Association between TNKS and BCR. A pulldown assay was performed with S protein beads (SFB-tagged BCR was used as the bait), and the indicated proteins were detected by WB.

(E) TNKS specifically binds to STRN3 in the STRIPAK complex. A pulldown assay was performed with S protein beads (SFB-tagged proteins were used as the baits), and the indicated proteins were detected by WB.

(F) Association between TNKS/2 and STRN3. A pulldown assay was performed with S protein beads (SFB-tagged proteins were used as the baits), and the indicated proteins were detected by WB.

(G) Association between GSK3β and TNKS/2. A pulldown assay was performed with S protein beads (SFB-tagged TNKS/2 were used as the baits), and the indicated proteins were detected by WB.

(H and I) GSK3β stabilizes TNKS/2. Cells were treated with 25 mM LiCl for 12 hr and subjected to WB with the indicated antibodies (H). To assess dose dependency, we used 10 or 25 mM LiCl to treat cells for 12 hr (H). To assess the effects of XAV939 treatment, we pretreated cells with 10 μM XAV939 for 24 hr and then subjected them to treatment with 25 mM LiCl for another 12 hr (I). DMSO was used as a control for XAV939 treatment. Quantification of TNKS protein levels is shown as numbers below the blots.

(J) TNKS associates with PEX14, but not PEX5. A pulldown assay was performed with S protein beads (SFB-tagged proteins were used as the baits), and the indicated proteins were detected by WB. The labels "long" and "short" refer to the exposure time for WB.

(K) Both TNKS and TNKS2 associate with PEX14. A pulldown assay was performed with S protein beads (SFB-tagged TNKS/2 proteins were used as the baits), and the indicated proteins were detected by WB.

(legend continued on next page)

PEX14 (Figure 3L). Interestingly, of the four potential TNKS-binding motifs (TBMs) in PEX14 predicted in a previous study (Guettler et al., 2011) (Figure 3M), we found that both the third and fourth motifs were required for the association of PEX14 with TNKS (Figure 3N), suggesting that these two TBMs function cooperatively to mediate the association between PEX14 and TNKS. Together, these results demonstrated that PEX14 is a bona fide binding partner for TNKS and TNKS2.

TNKS and TNKS2 Localize on Peroxisomes

TNKS and TNKS2 have several different cellular localizations (Lehtiö et al., 2013; Riffell et al., 2012; Vyas et al., 2013), but they mostly form vesicle-like punctate structures in the cytoplasm (Figure 4A). Using different organelle markers as controls, we found that TNKS partially co-localized with the endoplasmic reticulum, but not with the Golgi apparatus, early endosomes, or mitochondria (Figure 4A). Because TNKS and TNKS2 associated with PEX14 (Figures 3J–3N), we next investigated whether TNKS and TNKS2 would co-localize with PEX14 on peroxisomes. Indeed, as shown in Figure 4B, both TNKS and TNKS2 co-localized with PEX14. Depletion of PEX14 TBMs (TBM3 and TBM4) disrupted the co-localization between TNKS and PEX14 (Figure S2A). In addition, the peroxisome localization of TNKS and TNKS2 was confirmed by using additional peroxisome markers, PMP70, PMP-N-10, and catalase (Figure 4B; Figure S2B). Taken together, this evidence suggests that TNKS and TNKS2 localize on peroxisomes.

TNKS and TNKS2 Promote Pexophagy

Interestingly, overexpression of TNKS or TNKS2 led to a decrease in the total number of peroxisomes in cells (Figures 5A and 5B) and the enlargement of individual peroxisomes (Figures 5A and 5C), where TNKS or TNKS2 co-localized with these enlarged peroxisomes. The cell size was not obviously changed in this experimental setting. It is known that the number of peroxisomes, like other metabolic organelles in cells, is highly regulated in the cell (Till et al., 2012). The reduction of the number of peroxisomes is mediated by pexophagy, a type of macroautophagy in which large cytosolic material is delivered to lysosomes for degradation (Iwata et al., 2006). An inability to maintain peroxisome numbers has been linked to neurodegenerative and developmental disorders (Ribeiro et al., 2012; Singh et al., 2009), but the precise mechanisms underlying pexophagy remain unclear. Our data of reduced peroxisome number and enlarged individual peroxisomes in cells with TNKS/2 overexpression suggested that TNKS and TNKS2 may promote pexophagy.

To confirm this finding, we examined the co-localization of TNKS and the autophagy marker LC3. As expected, the enlarged peroxisomes induced by TNKS co-localized with LC3 (Figure 5D). Because pexophagy requires the involvement of lysosomes, we next examined and showed that the TNKS-positive peroxisomes also co-localized with lysosomes (Figure 5D). Taken together, these results confirmed that TNKS and TNKS2 have roles in promoting pexophagy.

Intriguingly, the enzyme activities of TNKS/2 were not required for pexophagy; a TNKS-inactive mutant, TNKS-PD, promoted co-localization of the autophagy marker LC3 and peroxisomes (Figure 5D). Consistent with this finding, XAV939 treatment failed to block TNKS-induced co-localization of peroxisomes and LC3 (Figure 5D). Moreover, overexpression of the E3 ligase RNF146, which recognizes and degrades TNKS substrates, had no effect on peroxisome number (Figures S3A and S3B) or size (Figures S3A and S3C). Collectively, these data suggest that the enzyme activities of TNKS/2 are not essential for TNKS/2-induced pexophagy.

TNKS and TNKS2 Are Involved in Selective Pexophagy during Amino Acid Starvation

Under low-amino acid conditions, peroxisomes are degraded by selective pexophagy (Sargent et al., 2016). Treatment with Hank's balanced salt solution (HBSS), a medium that lacks amino acids but contains glucose for cell survival, induced pexophagy, as indicated by a decrease in expression levels of two peroxisome proteins, PMP70 and catalase (Figure 5E; Figure S3D). Interestingly, loss of TNKS/2 prevented HBSS-induced pexophagy, as indicated by the stabilization of peroxisome proteins PMP70 and catalase in HBSS-treated cells (Figure 5E; Figure S3D). Reconstitution of either TNKS or its inactive mutant TNKS-PD rescued HBSS-induced pexophagy in TNKS/2-deficient cells (Figure S3E). These data suggest that TNKS and TNKS2 are involved in HBSS-induced pexophagy.

Notably, the level of TNKS protein expression decreased upon treatment with HBSS (Figure 5E), suggesting that as a peroxisome-localized protein, TNKS could also be targeted for clearance via pexophagy. To test this hypothesis, we examined the TNKS level in cells treated with bafilomycin A1 (BFA), a vacuolar-type H+-ATPase (V-ATPase) inhibitor, which prevents maturation of autophagic vacuoles by inhibiting fusion between autophagosomes and lysosomes (Yamamoto et al., 1998). As shown in Figure S3F, treatment with BFA stabilized expression levels of TNKS and two peroxisome proteins (PMP70 and catalase) upon HBSS treatment.

However, HBSS-induced pexophagy was enhanced in cells pretreated with XAV939 (Figure 5F; Figure S3G), in which TNKS/2 protein levels were dramatically increased. Moreover, HBSS-induced starvation combined with XAV939 treatment further enhanced pexophagy over HBSS treatment only, as shown by the decreased peroxisome number (Figures 5G and 5H) and the enlarged peroxisome size (Figures 5G and 5I). Given that XAV939 is a TNKS/2 enzyme inhibitor, these results further demonstrated that TNKS and TNKS2 promote selective pexophagy independently of their enzyme activities.

(L) The association between TNKS and PEX14 is independent of TNKS enzyme activity. The SFB-tagged wild-type TNKS and its PAR-inactive mutant, TNKS-PD, were used in the pulldown assay.

(M and N) Two TNKS/2-binding motifs (TBMs) were identified in PEX14. Four TBMs were predicted (M), and TBM3 and TBM4 were required for the association between TNKS and PEX14 (N). A pulldown assay was performed with S protein beads (SFB-tagged PEX14 and its TBM-deletion mutants were used as the baits), and the indicated proteins were detected by WB. Quantification of TNKS in pulldown samples is shown as numbers below the blot.

See also Figure S2.

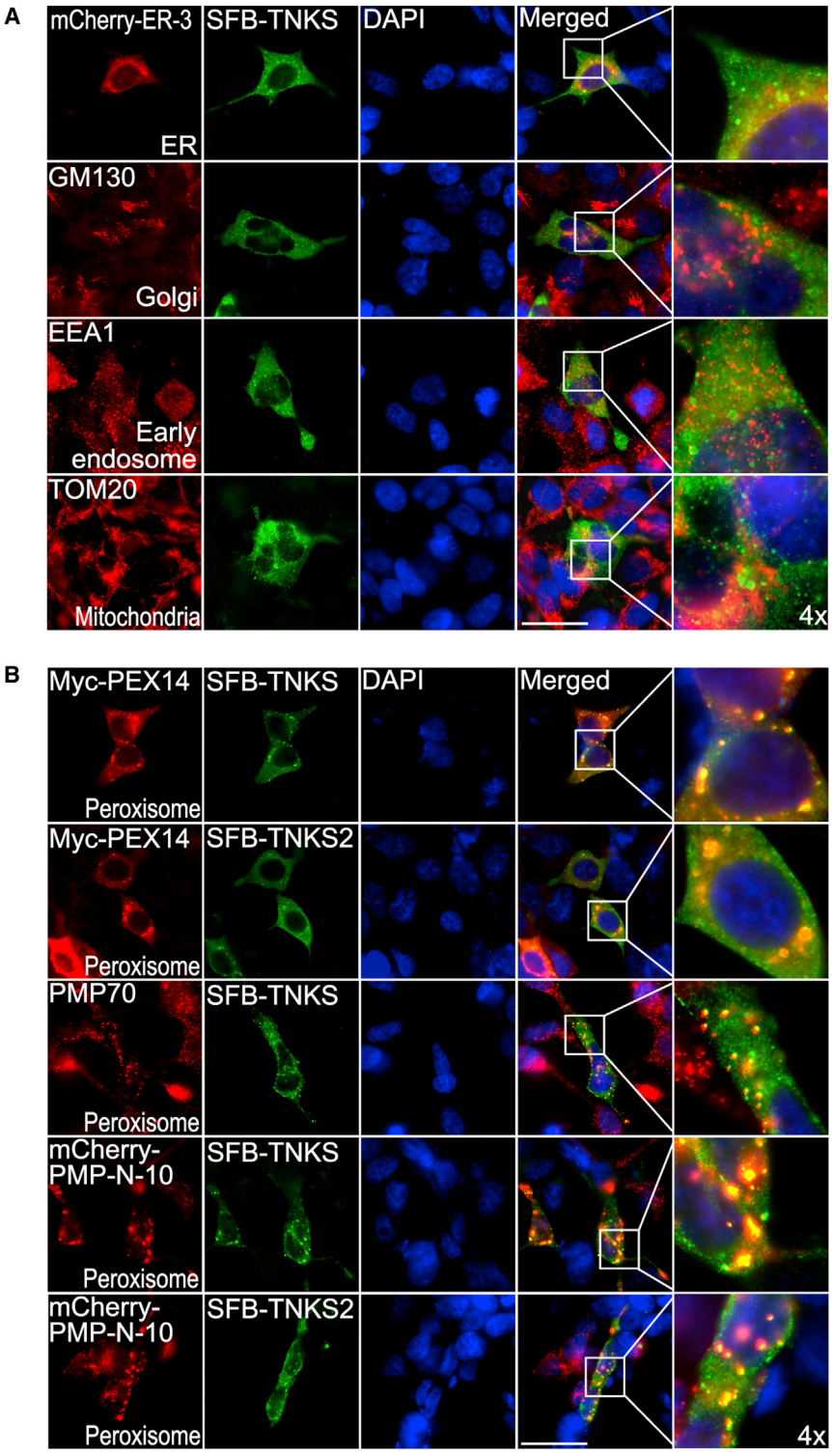

Figure 4. TNKS and TNKS2 Localize on Peroxisomes

(A) Formation of TNKS as vesicle-like structures in the cytoplasm. Immunofluorescent staining was performed to detect the localization of SFB-tagged TNKS with the indicated constructs or antibodies. Nuclei were stained with DAPI.

(B) TNKS/2 localize on peroxisomes. Immunofluorescent staining was performed to detect the localization of SFB-tagged TNKS/2 with the indicated constructs or antibody. Nuclei were stained with DAPI. PMP70 and PMP-N-10 are peroxisome markers.

EEA1, early endosome marker; ER-3, endoplasmic reticulum marker; GM130, Golgi marker; TOM20, mitochondria marker. Scale bars, 20 μm. See also Figure S2.

TNKS's Ankyrin Domain Is Required for Its Peroxisome Localization and Its Role in Pexophagy

To determine how TNKS and TNKS2 regulate pexophagy, we generated a series of TNKS domain-deletion mutants (Figure 6A). As shown in Figure 6B, loss of TNKS's ankyrin domain, but not its SAM or PARP domain, disrupted its peroxisome localization. Moreover, TNKS's ankyrin domain was also required for its role in promoting pexophagy, because overexpression of the TNKS ankyrin domain-deletion mutant did not affect either peroxisome number (Figures 6B and 6C) or peroxisome size (Figures 6B and 6D). On the other hand, deletion of either the SAM domain or the PARP domain of TNKS did not affect its peroxisome localization or its role in pexophagy (Figures 6A–6D). Because the ankyrin domain mediates the association between TNKS/2 and their binding partners, these results suggest that some TNKS/2-binding proteins are required for TNKS/2 peroxisome localization and their roles in pexophagy.

TNKS and TNKS2 Associate with the Autophagy-Related Protein ATG9A

Because TNKS and TNKS2 bind to PEX14 and localize in peroxisomes, we studied whether the TNKS/2 serve as a receptor for selective autophagy on peroxisomes. TNKS and PEX14 co-localized with both autophagy marker LC3 and lysosomes (Figure 6E). Previous studies showed that the autophagy receptors p62 and NBR1 are involved in pexophagy (Deosaran et al., 2013). However, we failed to detect the interactions between TNKS/2 and p62, NBR1, or LC3 (data not shown), suggesting that other autophagy-related proteins may bind to TNKS/2 and be required for TNKS-dependent pexophagy. To identify such candidate proteins, we searched the TNKS/2-HCIP list generated by our proteomic analysis and identified an autophagy-related protein, ATG9A,

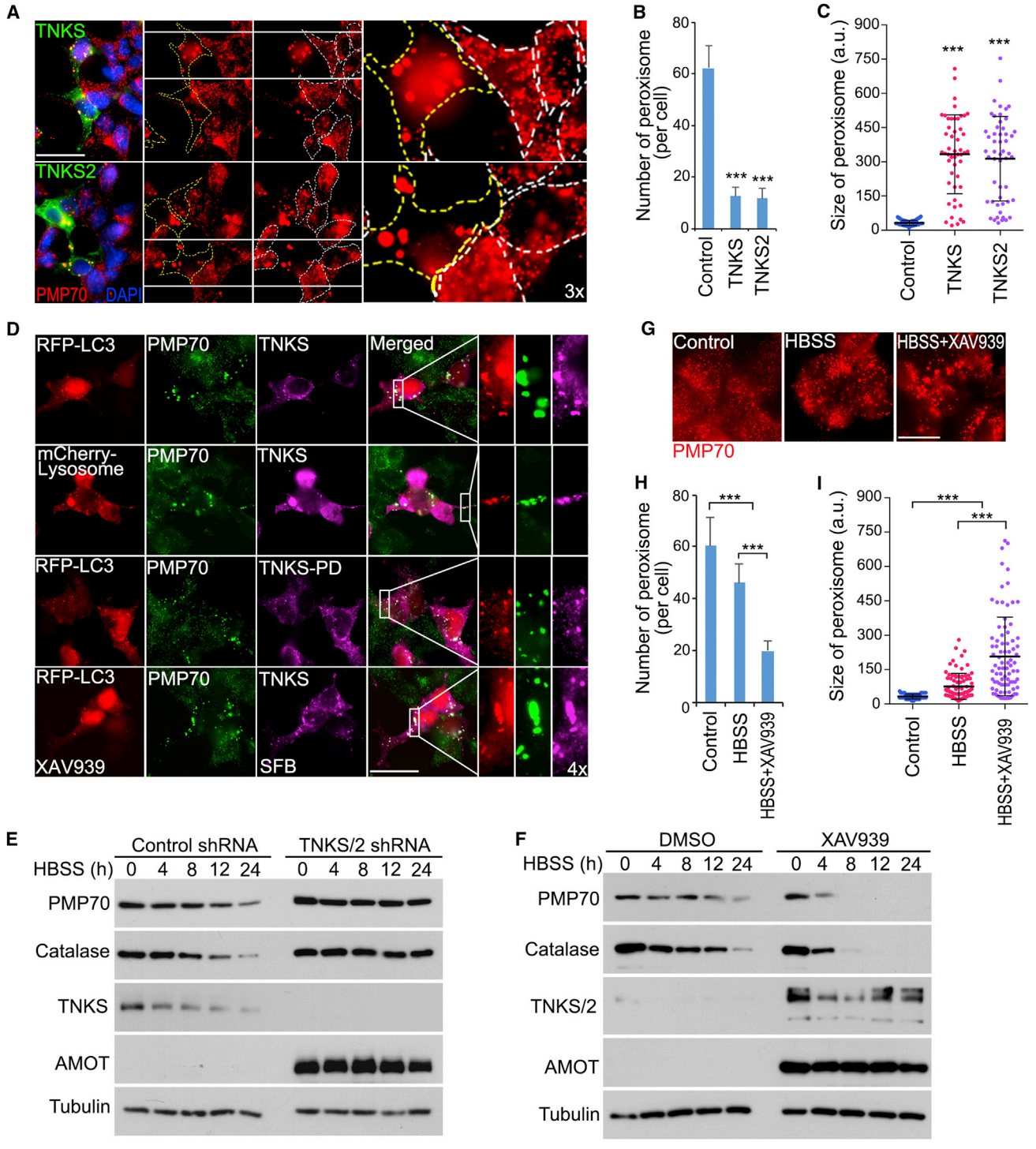

Figure 5. TNKS and TNKS2 Promote Pexophagy

(A–C) TNKS and TNKS2 changed the number and size of peroxisomes. Immunofluorescent staining was performed to detect the localization of SFB-tagged TNKS/2 and the peroxisome marker PMP70. Nuclei were stained with DAPI. TNKS-positive cells are indicated by the yellow line, and TNKS-negative cells are indicated by the white line. Gated areas are enlarged (A). The number of peroxisomes per TNKS-positive or -negative cell is shown (B). The size of each peroxisome was measured (C). Data are represented as mean ± SEM.

(D) TNKS promotes pexophagy independently of PAR activity. Immunofluorescent staining was performed to detect the localization of SFB-tagged TNKS and TNKS-PD with RFP-LC3, mCherry-lysosome, and PMP70 antibody. Cells were pretreated with XAV939 (10 μM) for 24 hr.

(legend continued on next page)

as a potential TNKS/2-binding protein in both the DMSO- and XAV939-treated groups (Figure 2).

Upon induction of autophagy, ATG9A co-localizes with phagophore markers in autophagosomes (Young et al., 2006). Functionally, ATG9A is the only multipass transmembrane ATG protein; it promotes autophagic membrane growth via a poorly defined mechanism (Noda et al., 2000; Young et al., 2006). Interestingly, ATG9A associated with TNKS/2 in our pulldown experiments (Figure 6F). Moreover, TNKS/2 and ATG9A co-localized in a vesicle-like structure in the cytoplasm in a manner similar to TNKS-positive peroxisome localization (Figure 6G). In addition, three TBMs were predicted in ATG9A (Figure S4A), the first of which was required for the association between TNKS and ATG9A (Figure S4B). Although ATG9A and PEX14 formed distinct vesicles in the cells (Figure 6H), overexpression of TNKS promoted their co-localization (Figure 6H). These results suggested that TNKS might link PEX14 with ATG9A to promote pexophagy.

To test this hypothesis, we generated short hairpin RNA (shRNA)-mediated knockdown cells for PEX14 and ATG9A, respectively (Figure 6I). Interestingly, loss of PEX14 disrupted the peroxisome localization of TNKS (Figure 6J) and inhibited TNKS-induced pexophagy; both the number and size of the peroxisomes were similar to those in untransfected cells (Figures 6K and 6L). In contrast, although TNKS was still able to localize on the peroxisomes (Figure 6J), it failed to induce pexophagy in ATG9A-deficient cells (Figure 6J); both the number and size of the peroxisomes were similar to those in untransfected cells (Figures 6J–6L). Moreover, loss of PEX14 or ATG9A stabilized the peroxisome proteins PMP70 and catalase in response to combination treatment with HBSS and XAV939 (Figure S4C); however, reconstitution of either PEX14 or ATG9A, but not their TBM-deleted mutants, rescued the pexophagy induced by combination treatment with HBSS and XAV939 (Figure S4C). Taken together, these results demonstrated that an ATG9A-TNKS/2-PEX14 complex may serve as a receptor to induce pexophagy, where TNKS and TNKS2 promote pexophagy by associating with PEX14 on the peroxisomes and recruiting autophagy machinery through ATG9A (Figure 6M).

DISCUSSION

In this study, we analyzed the human TNKS/2 protein interaction network, identified more than 100 HCIPs for TNKS/2, and expanded our knowledge of the cellular functions of TNKS/2. Because many TNKS substrates can be recognized by the E3 ligase RNF146 and targeted via proteasome-dependent degradation, the TNKS inhibitor XAV939 was used to stabilize the TNKS substrates in cells stably expressing TNKS or TNKS2, which increased the chance of identifying TNKS substrates in our TAP-MS experiments. Of note, at the TNKS inhibitor XAV939 concentration (10 μM) used here, other PARP proteins such as PARP1, PARP2, and PARP3 are expected to be inhibited as well.

Through GO analysis, these identified HCIPs were parsed into categories associated with their biological functions, providing a useful resource for further dissecting the cellular roles of TNKS/2. Future investigation is required to elucidate the functional significance of the HCIPs identified here. For example, we found that an E3 ligase group (RNF146 and five other E3 ligases) was highly enriched in association with TNKS/2 in DMSO-treated control cells (Figure 2). RNF146 is known to bind to TNKS/2 through the WWE domain of RNF146 and the auto-PARylation of TNKS/2 (Zhang et al., 2011). XAV939-based treatment inhibited PARylation, and therefore disrupted the association of TNKS/2 with RNF146. Whether the other five E3 ligases function similarly and/or redundantly to RNF146 deserves further investigation.

TNKS and TNKS2 have multiple cellular localizations, such as at the telomeres (Smith et al., 1998), centrosomes (Ozaki et al., 2012), and Golgi apparatus (Chi and Lodish, 2000). Although our proteomic analysis revealed TNKS/2-related HCIPs in these cellular compartments, confirming previously reported findings (Figure 2), our localization study indicated that a significant fraction of TNKS and TNKS2 localize to vesicle-like structures in the cytoplasm (Figure 4A). Furthermore, our functional studies revealed that TNKS and TNKS2 associate with peroxisome protein PEX14 and localize on peroxisomes (Figures 3K, 4B, and S2B).

Intriguingly, our study uncovered an unexpected mechanism of pexophagy mediated by TNKS/2. In mammalian cells, the peroxisomes and other cytosolic components, including damaged mitochondria, the endoplasmic reticulum, aggregated proteins, and membrane remnants, are substrates of selective autophagy and are sequestered and degraded in lysosomes (Monastyrska and Klionsky, 2006; Sakai et al., 2006). As the initial step of autophagy, a nascent membrane forms in the cytoplasm and wraps around these targeted cytosolic components (protein aggregates, organelle, membrane remnants) to form the autophagosome, a large double-membrane-bounded structure. Autophagosome fuses with lysosome, which allows the sequestered materials to be degraded in lysosomes, recycled as free amino acids, lipids, and other small molecules, and utilized by the cell. Many autophagy receptors link organelles with autophagosomes by associating with autophagy protein LC3 on autophagosomes and ubiquitin substrate on the organelle (Rogov et al., 2014; Zaffagnini and Martens, 2016). The ubiquitination of peroxisome membrane proteins initiates the recognition of peroxisomes for degradation (Kim et al., 2008). Two

(E) TNKS and TNKS2 are involved in HBSS-induced pexophagy. HEK293A cells transduced with either control shRNA or TNKS/2 shRNAs were treated with HBSS for the indicated times. WB was performed with the indicated antibodies.
(F) XAV939 treatment promotes HBSS-induced pexophagy. HEK293A cells were pretreated with either DMSO or XAV939 (10 μM) for 24 hr and then treated with HBSS for the indicated times. WB was performed with the indicated antibodies.
(G–I) Combined treatment with XAV939 and HBSS induces pexophagy. HEK293A cells were treated with HBSS only or HBSS containing 10 μM XAV939 for 24 hr and then subjected to immunofluorescent assays with a PMP70 antibody (G). The number of peroxisomes per cell is shown (H). The size of each peroxisome was measured (I). Data are represented as mean ± SEM.
Scale bars, 20 μm. ***$p < 0.001$. a.u., arbitrary unit. See also Figure S3.

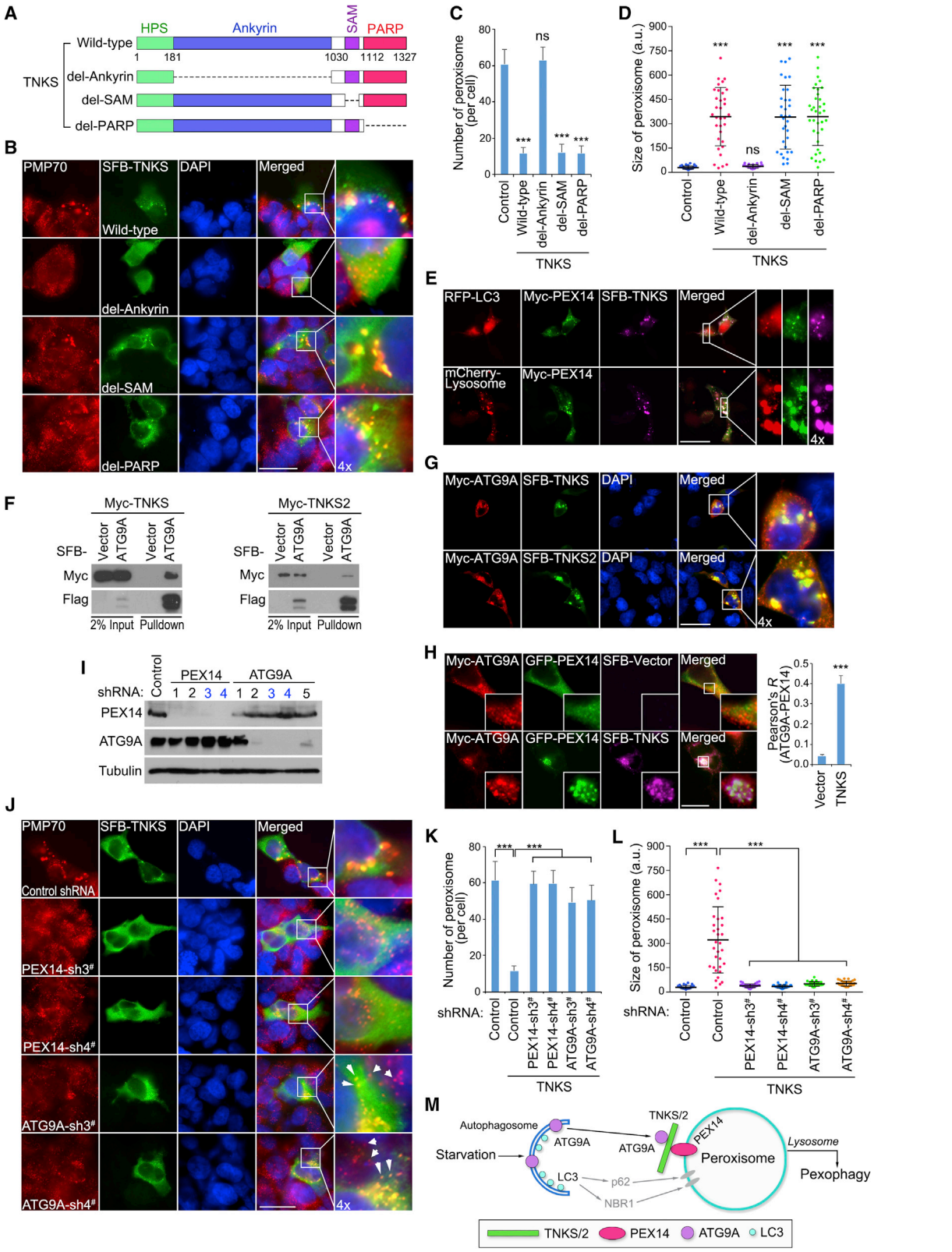

(legend on next page)

ubiquitin-binding autophagy receptors, NBR1 and p62, are recruited to target the ubiquitinated peroxisomes to autophagosomes for degradation (Deosaran et al., 2013; Walter et al., 2014; Yamashita et al., 2014). The peroxisomal biogenesis factor 5 (PEX5) has been identified to be ubiquitinated and involved in pexophagy (Nordgren et al., 2015; Zhang et al., 2015). In addition, PEX2 was found to have E3 ubiquitin ligase activity and promote the ubiquitination of peroxisome membrane proteins (i.e., PEX5 and PMP70) in pexophagy (Sargent et al., 2016). Intriguingly, the TNKS/2-mediated pexophagy mechanism discovered in this study is a non-canonical process. On one hand, TNKS and TNKS2 are not ubiquitin-binding proteins but require a physical protein-protein interaction with PEX14 to localize on the peroxisome (Figure 6M). On the other hand, TNKS and TNKS2 are not autophagy-related proteins but need ATG9A to recruit the autophagy machinery to peroxisomes (Figure 6M). Our study uncovered a ubiquitination-independent mechanism for pexophagy, in which the ATG9A-TNKS/2-PEX14 axis bridges the peroxisome and autophagy machinery to induce pexophagy. The detailed regulatory mechanism of this process deserves further experimentation. Moreover, examining whether dysregulation of TNKS/2 is involved in the development of neurodegenerative and developmental disorders caused by peroxisome clearance will be interesting.

Notably, TNKS/2 enzyme activities are not required for pexophagy, although we have demonstrated that PEX14 is a substrate of TNKS/2 (data not shown). This raises the possibility that TNKS and TNKS2 function independently of their PAR activities but require association with their binding partners. Given that GSK3β stabilized TNKS/2 (Figures 3H and 3I) and is involved in mTOR inhibition (Inoki et al., 2006), which subsequently promotes autophagy, we speculate that GSK3β may play a critical role in TNKS/2-mediated pexophagy. This detailed regulatory mechanism deserves further investigation. Collectively, our proteomic study not only identified biologically relevant functions for TNKS/2, but also provided a rich resource for further exploration of their functions in numerous cellular processes.

EXPERIMENTAL PROCEDURES

The information about antibodies and chemicals, constructs and viruses, cell culture and transfection, immunofluorescent staining, and MS analysis in this study is described in the Supplemental Experimental Procedures.

TAP of SFB-Tagged Protein Complexes

HEK293T cells stably expressing SFB-fused TNKS and TNKS2 proteins were selected by culturing in medium containing 2 μg/mL puromycin and confirmed by immunostaining and WB as described previously (Wang et al., 2014). For TAP, HEK293T cells that had been pretreated with DMSO or 10 μM XAV939 for 48 hr were lysed in 100 mM NaCl; 20 mM Tris-Cl, pH 8.0; 0.5 mM EDTA; 0.5% Nonidet P-40 (NETN) buffer (with protease inhibitors) at 4°C for 20 min. The crude lysates were centrifugated at 14,000 rpm for 15 min at 4°C. The supernatants were incubated with streptavidin-conjugated beads (Amersham) for 1 hr at 4°C. The beads were washed three times with NETN buffer, and bound proteins were eluted with NETN buffer containing 2 mg/mL biotin (Sigma) for 120 min at 4°C. The elutes were incubated with S protein beads (Novagen) for 1 hr. The beads were washed three times with NETN buffer and subjected to SDS-PAGE. Each pulldown sample was run just into the separation gel so that the whole band could be excised as one sample and subjected to in-gel trypsin digestion and MS analysis.

For reciprocal TAP-MS analysis, HEK293T cells stably expressing SFB-tagged indicated bait proteins were established by viral infection and puromycin selection. After validation of bait protein expression and localization, stable cells were pretreated with 10 μM XAV939 for 48 hr and subjected to TAP-MS.

Bioinformatic Analysis

We performed the data analysis using the MUSE algorithm as previously described (Li et al., 2016) to assign quality scores to the identified protein-protein interactions. 1,626 unrelated TAP-MS experiments, which were performed under identical experimental conditions (1,606 experiments using overexpressed TAP-tagged protein baits and 20 experiments using empty vector baits), were used as controls for MUSE analysis. We assigned a MUSE score to each identified interaction and considered any interaction with a MUSE score of least 0.8 and raw spectra counts greater than 1 to be an HCIP. We also used a subset of these 1,626 controls, which consists of 338 TAP-MS experiments performed under the same conditions as the raw data available in the PRIDE database (PRIDE: PXD000415, PXD000593/293T, PXD001383, and PXD002462), as our secondary control set and then performed MUSE analysis again. To compare our HCIP dataset with the

Figure 6. PEX14 and ATG9A Are Required for TNKS/2-Induced Pexophagy

(A) Schematic illustration of TNKS domain-deletion mutants.

(B–D) Loss of the ankyrin domain inhibits TNKS-induced pexophagy. Constructs encoding wild-type or TNKS domain-deletion mutants were transfected into HEK293A cells. Immunofluorescent staining was performed by using PMP70 and FLAG antibodies (B). The number of peroxisomes per FLAG-positive or FLAG-negative cell is shown (C). The size of each peroxisome was measured (D). Data are represented as mean ± SEM.

(E) TNKS and PEX14 co-localized with LC3 and lysosomes.

(F) Association between TNKS/2 and ATG9A. A pulldown assay was performed with S protein beads (SFB-tagged ATG9A was used as the bait), and the indicated proteins were detected by WB.

(G) TNKS and TNKS2 co-localize with ATG9A in vesicle-like structures.

(H) TNKS promotes co-localization of ATG9A and PEX14. Immunofluorescent staining was performed to detect the localization of the indicated proteins. Pearson's correlation coefficient (*R*) for ATG9A and PEX14 was determined by using ImageJ software. Data are represented as mean ± SEM.

(I) shRNA-mediated downregulation of PEX14 and ATG9A. HEK293A cells stably transduced with the indicated shRNAs were subjected to WB with indicated antibodies. Two shRNAs targeting PEX14 (lanes 3 and 4) or ATG9A (lanes 3 and 4) that showed high knockdown efficiency were chosen for functional studies and are labeled in blue.

(J–L) Loss of PEX14 or ATG9A blocks TNKS-induced pexophagy. Construct encoding SFB-tagged TNKS was transfected into HEK293A cells stably transduced with the indicated shRNAs. Immunofluorescent staining was performed using PMP70 and FLAG antibodies (J). Nuclei were stained with DAPI. The number of peroxisomes per FLAG-positive or FLAG-negative cell is shown (K). The size of each peroxisome was measured (L). Short arrows indicate the peroxisomes in untransfected control cells. Long arrows indicate the peroxisomes in transfected cells. Data are represented as mean ± SEM.

(M) Schematic illustration of TNKS/2-mediated pexophagy. Under the starved condition, TNKS/2 localize on peroxisomes and recruit autophagy machinery to peroxisomes. This process is mediated by two TNKS1/2-associated proteins, PEX14 and ATG9A, on peroxisomes and autophagy machinery, respectively. Formed autophagosome fuses with lysosome, where peroxisomal proteins are degraded and recycled in the cell.

Scale bars, 10 μm (H); 20 μm (B, E, G, and J). ***$p < 0.001$. a.u., arbitrary unit; ns, no significance. See also Figure S4.

CRAPome dataset, we collected the results of 329 experiments performed in HEK293(T) cells in the CRAPome database (V1.1, 2014.1, *H. sapiens*) to estimate the prey frequency and abundance information.

The TNKS/2 interactome was enriched in the signaling pathway using the HCIP sets. The p values were estimated using the Knowledge Base provided by Ingenuity Pathway software (Ingenuity Systems, https://www.ingenuity.com), which contains findings and annotations from multiple sources including the GO database, KEGG pathway database, and Panther pathway database. Only statistically significant correlations ($p < 0.05$) are shown. The −log (p value) for each function and related HCIPs is listed.

ACCESSION NUMBERS

The accession number for the MS proteomic data reported in this paper is ProteomeXchange Consortium PRIDE: PXD004647 (Vizcaíno et al., 2013) (http://proteomecentral.proteomexchange.org). The detailed project information is as follows: project name, Human Tankyrases TAP-LC-MSMS; project accession number PRIDE: PXD004647; and project http://dx.doi.org/10.6019/PXD004647.

SUPPLEMENTAL INFORMATION

Supplemental Information includes Supplemental Experimental Procedures, four figures, and six tables and can be found with this article online at http://dx.doi.org/10.1016/j.celrep.2017.06.077.

AUTHOR CONTRIBUTIONS

X.L., J.C., and W.W. conceived the experiments. H.H., M.-T.Z., B.Y., A.P.T., N.L., and W.W. performed all of the experiments. X.L. and W.W. performed the bioinformatic analysis. W.W., X.L., and J.C. wrote the manuscript.

ACKNOWLEDGMENTS

W.W. thanks J.C. for his mentoring and continuous support. We also thank Drs. Steven Gygi and Ross Tomaino (Taplin Mass Spectrometry Facility, Harvard Medical School) for help with the mass spectrometry analysis, Dr. Aimee Edinger (University of California, Irvine) for the technical help, Dr. Amy Ninetto (MD Anderson Cancer Center) for editing the manuscript, and Dr. Yutong Sun and the staff of the shRNA-ORFeome core facility at MD Anderson Cancer Center for the open reading frames (ORFs) and shRNAs. W.W. is a recipient of an American Association for Cancer Research Career Development Award for Translational Breast Cancer Research supported by the Breast Cancer Research Foundation (grant 16-20-26-WANG). This work was supported in part by a Department of Defense Era of Hope research scholar award (W81XWH-09-1-0409 to J.C.) and an American Cancer Society Institutional Research Grant (to W.W.). W.W. is a member of the Chao Family Comprehensive Cancer Center (grant P30 CA062203) and the Center for Complex Biological Systems (P50-GM076516) at UC Irvine.

Received: January 28, 2017
Revised: May 12, 2017
Accepted: June 23, 2017
Published: July 18, 2017

REFERENCES

Amé, J.C., Spenlehauer, C., and de Murcia, G. (2004). The PARP superfamily. BioEssays *26*, 882–893.

Berger, F., Ramírez-Hernández, M.H., and Ziegler, M. (2004). The new life of a centenarian: signalling functions of NAD(P). Trends Biochem. Sci. *29*, 111–118.

Brocard, C., Lametschwandtner, G., Koudelka, R., and Hartig, A. (1997). Pex14p is a member of the protein linkage map of Pex5p. EMBO J. *16*, 5491–5500.

Bürkle, A. (2005). Poly(ADP-ribose). The most elaborate metabolite of NAD+. FEBS J. *272*, 4576–4589.

Chang, P., Jacobson, M.K., and Mitchison, T.J. (2004). Poly(ADP-ribose) is required for spindle assembly and structure. Nature *432*, 645–649.

Chang, W., Dynek, J.N., and Smith, S. (2005). NuMA is a major acceptor of poly(ADP-ribosyl)ation by tankyrase 1 in mitosis. Biochem. J. *391*, 177–184.

Chi, N.W., and Lodish, H.F. (2000). Tankyrase is a golgi-associated mitogen-activated protein kinase substrate that interacts with IRAP in GLUT4 vesicles. J. Biol. Chem. *275*, 38437–38444.

Chiang, Y.J., Hsiao, S.J., Yver, D., Cushman, S.W., Tessarollo, L., Smith, S., and Hodes, R.J. (2008). Tankyrase 1 and tankyrase 2 are essential but redundant for mouse embryonic development. PLoS ONE *3*, e2639.

Deosaran, E., Larsen, K.B., Hua, R., Sargent, G., Wang, Y., Kim, S., Lamark, T., Jauregui, M., Law, K., Lippincott-Schwartz, J., et al. (2013). NBR1 acts as an autophagy receptor for peroxisomes. J. Cell Sci. *126*, 939–952.

Durkacz, B.W., Omidiji, O., Gray, D.A., and Shall, S. (1980). (ADP-ribose)n participates in DNA excision repair. Nature *283*, 593–596.

Durkacz, B.W., Irwin, J., and Shall, S. (1981a). Inhibition of (ADP-ribose)n biosynthesis retards DNA repair but does not inhibit DNA repair synthesis. Biochem. Biophys. Res. Commun. *101*, 1433–1441.

Durkacz, B.W., Shall, S., and Irwin, J. (1981b). The effect of inhibition of (ADP-ribose)n biosynthesis on DNA repair assayed by the nucleoid technique. Eur. J. Biochem. *121*, 65–69.

Guettler, S., LaRose, J., Petsalaki, E., Gish, G., Scotter, A., Pawson, T., Rottapel, R., and Sicheri, F. (2011). Structural basis and sequence rules for substrate recognition by Tankyrase explain the basis for cherubism disease. Cell *147*, 1340–1354.

Hottiger, M.O., Hassa, P.O., Lüscher, B., Schüler, H., and Koch-Nolte, F. (2010). Toward a unified nomenclature for mammalian ADP-ribosyltransferases. Trends Biochem. Sci. *35*, 208–219.

Huang, S.M., Mishina, Y.M., Liu, S., Cheung, A., Stegmeier, F., Michaud, G.A., Charlat, O., Wiellette, E., Zhang, Y., Wiessner, S., et al. (2009). Tankyrase inhibition stabilizes axin and antagonizes Wnt signalling. Nature *461*, 614–620.

Inoki, K., Ouyang, H., Zhu, T., Lindvall, C., Wang, Y., Zhang, X., Yang, Q., Bennett, C., Harada, Y., Stankunas, K., et al. (2006). TSC2 integrates Wnt and energy signals via a coordinated phosphorylation by AMPK and GSK3 to regulate cell growth. Cell *126*, 955–968.

Iwata, J., Ezaki, J., Komatsu, M., Yokota, S., Ueno, T., Tanida, I., Chiba, T., Tanaka, K., and Kominami, E. (2006). Excess peroxisomes are degraded by autophagic machinery in mammals. J. Biol. Chem. *281*, 4035–4041.

Kim, P.K., Hailey, D.W., Mullen, R.T., and Lippincott-Schwartz, J. (2008). Ubiquitin signals autophagic degradation of cytosolic proteins and peroxisomes. Proc. Natl. Acad. Sci. USA *105*, 20567–20574.

Koh, D.W., Dawson, T.M., and Dawson, V.L. (2005). Mediation of cell death by poly(ADP-ribose) polymerase-1. Pharmacol. Res. *52*, 5–14.

Kraus, W.L., and Lis, J.T. (2003). PARP goes transcription. Cell *113*, 677–683.

Lehtiö, L., Chi, N.W., and Krauss, S. (2013). Tankyrases as drug targets. FEBS J. *280*, 3576–3593.

Leung, A.K., Vyas, S., Rood, J.E., Bhutkar, A., Sharp, P.A., and Chang, P. (2011). Poly(ADP-ribose) regulates stress responses and microRNA activity in the cytoplasm. Mol. Cell *42*, 489–499.

Levaot, N., Voytyuk, O., Dimitriou, I., Sircoulomb, F., Chandrakumar, A., Deckert, M., Krzyzanowski, P.M., Scotter, A., Gu, S., Janmohamed, S., et al. (2011). Loss of Tankyrase-mediated destruction of 3BP2 is the underlying pathogenic mechanism of cherubism. Cell *147*, 1324–1339.

Li, N., Zhang, Y., Han, X., Liang, K., Wang, J., Feng, L., Wang, W., Songyang, Z., Lin, C., Yang, L., et al. (2015). Poly-ADP ribosylation of PTEN by tankyrases promotes PTEN degradation and tumor growth. Genes Dev. *29*, 157–170.

Li, X., Tran, K.M., Aziz, K.E., Sorokin, A.V., Chen, J., and Wang, W. (2016). Defining the protein-protein interaction network of the human protein tyrosine phosphatase family. Mol. Cell. Proteomics *15*, 3030–3044.

Malanga, M., and Althaus, F.R. (2005). The role of poly(ADP-ribose) in the DNA damage signaling network. Biochem. Cell Biol. *83*, 354–364.

Mariotti, L., Templeton, C.M., Ranes, M., Paracuellos, P., Cronin, N., Beuron, F., Morris, E., and Guettler, S. (2016). Tankyrase requires SAM domain-dependent polymerization to support Wnt-β-catenin signaling. Mol. Cell *63*, 498–513.

Mellacheruvu, D., Wright, Z., Couzens, A.L., Lambert, J.P., St-Denis, N.A., Li, T., Miteva, Y.V., Hauri, S., Sardiu, M.E., Low, T.Y., et al. (2013). The CRAPome: a contaminant repository for affinity purification-mass spectrometry data. Nat. Methods *10*, 730–736.

Monastyrska, I., and Klionsky, D.J. (2006). Autophagy in organelle homeostasis: peroxisome turnover. Mol. Aspects Med. *27*, 483–494.

Morrone, S., Cheng, Z., Moon, R.T., Cong, F., and Xu, W. (2012). Crystal structure of a Tankyrase-Axin complex and its implications for Axin turnover and Tankyrase substrate recruitment. Proc. Natl. Acad. Sci. USA *109*, 1500–1505.

Noda, T., Kim, J., Huang, W.P., Baba, M., Tokunaga, C., Ohsumi, Y., and Klionsky, D.J. (2000). Apg9p/Cvt7p is an integral membrane protein required for transport vesicle formation in the Cvt and autophagy pathways. J. Cell Biol. *148*, 465–480.

Nordgren, M., Francisco, T., Lismont, C., Hennebel, L., Brees, C., Wang, B., Van Veldhoven, P.P., Azevedo, J.E., and Fransen, M. (2015). Export-deficient monoubiquitinated PEX5 triggers peroxisome removal in SV40 large T antigen-transformed mouse embryonic fibroblasts. Autophagy *11*, 1326–1340.

Ozaki, Y., Matsui, H., Asou, H., Nagamachi, A., Aki, D., Honda, H., Yasunaga, S., Takihara, Y., Yamamoto, T., Izumi, S., et al. (2012). Poly-ADP ribosylation of Miki by tankyrase-1 promotes centrosome maturation. Mol. Cell *47*, 694–706.

Ribeiro, D., Castro, I., Fahimi, H.D., and Schrader, M. (2012). Peroxisome morphology in pathology. Histol. Histopathol. *27*, 661–676.

Riffell, J.L., Lord, C.J., and Ashworth, A. (2012). Tankyrase-targeted therapeutics: expanding opportunities in the PARP family. Nat. Rev. Drug Discov. *11*, 923–936.

Rogov, V., Dötsch, V., Johansen, T., and Kirkin, V. (2014). Interactions between autophagy receptors and ubiquitin-like proteins form the molecular basis for selective autophagy. Mol. Cell *53*, 167–178.

Rouleau, M., Patel, A., Hendzel, M.J., Kaufmann, S.H., and Poirier, G.G. (2010). PARP inhibition: PARP1 and beyond. Nat. Rev. Cancer *10*, 293–301.

Sakai, Y., Oku, M., van der Klei, I.J., and Kiel, J.A. (2006). Pexophagy: autophagic degradation of peroxisomes. Biochim. Biophys. Acta *1763*, 1767–1775.

Sargent, G., van Zutphen, T., Shatseva, T., Zhang, L., Di Giovanni, V., Bandsma, R., and Kim, P.K. (2016). PEX2 is the E3 ubiquitin ligase required for pexophagy during starvation. J. Cell Biol. *214*, 677–690.

Schreiber, V., Dantzer, F., Ame, J.C., and de Murcia, G. (2006). Poly(ADP-ribose): novel functions for an old molecule. Nat. Rev. Mol. Cell Biol. *7*, 517–528.

Singh, I., Singh, A.K., and Contreras, M.A. (2009). Peroxisomal dysfunction in inflammatory childhood white matter disorders: an unexpected contributor to neuropathology. J. Child Neurol. *24*, 1147–1157.

Smith, J.J., and Aitchison, J.D. (2013). Peroxisomes take shape. Nat. Rev. Mol. Cell Biol. *14*, 803–817.

Smith, S., Giriat, I., Schmitt, A., and de Lange, T. (1998). Tankyrase, a poly(ADP-ribose) polymerase at human telomeres. Science *282*, 1484–1487.

Till, A., Lakhani, R., Burnett, S.F., and Subramani, S. (2012). Pexophagy: the selective degradation of peroxisomes. Int. J. Cell Biol. *2012*, 512721.

Troilo, A., Benson, E.K., Esposito, D., Garibsingh, R.A., Reddy, E.P., Mungamuri, S.K., and Aaronson, S.A. (2016). Angiomotin stabilization by tankyrase inhibitors antagonizes constitutive TEAD-dependent transcription and proliferation of human tumor cells with Hippo pathway core component mutations. Oncotarget *7*, 28765–28782.

Vizcaíno, J.A., Côté, R.G., Csordas, A., Dianes, J.A., Fabregat, A., Foster, J.M., Griss, J., Alpi, E., Birim, M., Contell, J., et al. (2013). The PRoteomics IDEntifications (PRIDE) database and associated tools: status in 2013. Nucleic Acids Res. *41*, D1063–D1069.

Vyas, S., Chesarone-Cataldo, M., Todorova, T., Huang, Y.H., and Chang, P. (2013). A systematic analysis of the PARP protein family identifies new functions critical for cell physiology. Nat. Commun. *4*, 2240.

Walter, K.M., Schönenberger, M.J., Trötzmüller, M., Horn, M., Elsässer, H.P., Moser, A.B., Lucas, M.S., Schwarz, T., Gerber, P.A., Faust, P.L., et al. (2014). Hif-2α promotes degradation of mammalian peroxisomes by selective autophagy. Cell Metab. *20*, 882–897.

Wang, W., Li, X., Huang, J., Feng, L., Dolinta, K.G., and Chen, J. (2014). Defining the protein-protein interaction network of the human hippo pathway. Mol. Cell. Proteomics *13*, 119–131.

Wang, W., Li, N., Li, X., Tran, M.K., Han, X., and Chen, J. (2015). Tankyrase inhibitors target YAP by stabilizing angiomotin family proteins. Cell Rep. *13*, 524–532.

Wang, H., Lu, B., Castillo, J., Zhang, Y., Yang, Z., McAllister, G., Lindeman, A., Reece-Hoyes, J., Tallarico, J., Russ, C., et al. (2016). Tankyrase inhibitor sensitizes lung cancer cells to endothelial growth factor receptor (EGFR) inhibition via stabilizing angiomotins and inhibiting YAP signaling. J. Biol. Chem. *291*, 15256–15266.

Yamamoto, A., Tagawa, Y., Yoshimori, T., Moriyama, Y., Masaki, R., and Tashiro, Y. (1998). Bafilomycin A1 prevents maturation of autophagic vacuoles by inhibiting fusion between autophagosomes and lysosomes in rat hepatoma cell line, H-4-II-E cells. Cell Struct. Funct. *23*, 33–42.

Yamashita, S., Abe, K., Tatemichi, Y., and Fujiki, Y. (2014). The membrane peroxin PEX3 induces peroxisome-ubiquitination-linked pexophagy. Autophagy *10*, 1549–1564.

Yeh, T.Y., Sbodio, J.I., and Chi, N.W. (2006). Mitotic phosphorylation of tankyrase, a PARP that promotes spindle assembly, by GSK3. Biochem. Biophys. Res. Commun. *350*, 574–579.

Young, A.R., Chan, E.Y., Hu, X.W., Köchl, R., Crawshaw, S.G., High, S., Hailey, D.W., Lippincott-Schwartz, J., and Tooze, S.A. (2006). Starvation and ULK1-dependent cycling of mammalian Atg9 between the TGN and endosomes. J. Cell Sci. *119*, 3888–3900.

Zaffagnini, G., and Martens, S. (2016). Mechanisms of selective autophagy. J. Mol. Biol. *428* (*9 Pt A*), 1714–1724.

Zhang, Y., Liu, S., Mickanin, C., Feng, Y., Charlat, O., Michaud, G.A., Schirle, M., Shi, X., Hild, M., Bauer, A., et al. (2011). RNF146 is a poly(ADP-ribose)-directed E3 ligase that regulates axin degradation and Wnt signalling. Nat. Cell Biol. *13*, 623–629.

Zhang, J., Tripathi, D.N., Jing, J., Alexander, A., Kim, J., Powell, R.T., Dere, R., Tait-Mulder, J., Lee, J.H., Paull, T.T., et al. (2015). ATM functions at the peroxisome to induce pexophagy in response to ROS. Nat. Cell Biol. *17*, 1259–1269.